

EUROPEAN LABORATORY FOR PARTICLE PHYSICS

Charm Program of NA61/SHINE: Motivation and Measurements¹



**Aleksandra Snoch
and the NA61/SHINE Collaboration**

<http://na61.web.cern.ch/>

Abstract

Recently, the NA61/SHINE experiment at the CERN SPS has extended its program on physics of strong interactions by measurements of charm hadron production in nucleus-nucleus collisions. This charm program is here briefly summarized.

April 7, 2024

¹Invited talk presented at the ECT* Workshop on Phase Diagram of Strongly Interacting Matter: From Lattice QCD to Heavy-Ion Collision Experiments, Trento, Italy, November 27, 2017, and Reimei Workshop on Hadronic Resonances and Dense Nuclear Matter, Tokai, Japan, December 11, 2017

The NA61/SHINE Collaboration

A. Aduszkiewicz¹⁶, Y. Ali¹³, E.V. Andronov²², T. Antičić³, B. Baatar²⁰, M. Baszczyk¹⁴, S. Bhosale¹¹, A. Blondel²⁵, M. Bogomilov², A. Brandin²¹, A. Bravar²⁵, W. Bryliński¹⁸, J. Brzychczyk¹³, S.A. Bunyatov²⁰, O. Busygina¹⁹, A. Bzdak¹⁴, H. Cherif⁷, M. Ćirković²³, T. Czopowicz¹⁸, A. Damyanova²⁵, N. Davis¹¹, M. Deveaux⁷, W. Dominik¹⁶, P. Dorosz¹⁴, J. Dumarchez⁴, R. Engel⁵, A. Ereditato²⁴, G.A. Feofilov²², Z. Fodor^{8,17}, C. Francois²⁴, A. Garibov¹, M. Gaździcki^{7,10}, M. Golubeva¹⁹, K. Grebieszko¹⁸, F. Guber¹⁹, A. Haesler²⁵, A.E. Hervé⁵, J. Hysten²⁶, S.N. Igoekin²², A. Ivashkin¹⁹, S.R. Johnson²⁸, K. Kadija³, E. Kaptur¹⁵, M. Kielbowicz¹¹, V.A. Kireyeu²⁰, V. Klochov⁷, V.I. Kolesnikov²⁰, D. Kolev², A. Korzenev²⁵, V.N. Kovalenko²², K. Kowalik¹², S. Kowalski¹⁵, M. Koziel⁷, A. Krasnoperov²⁰, W. Kucewicz¹⁴, M. Kuich¹⁶, A. Kurepin¹⁹, D. Larsen¹³, A. László⁸, T.V. Lazareva²², M. Lewicki¹⁷, B. Lundberg²⁶, B. Łysakowski¹⁵, V.V. Lyubushkin²⁰, M. Mačkowiak-Pawłowska¹⁸, B. Maksiak¹⁸, A.I. Malakhov²⁰, D. Manić²³, A. Marchionni²⁶, A. Marcinek¹¹, A.D. Marino²⁸, K. Marton⁸, H.-J. Mathes⁵, T. Matulewicz¹⁶, V. Matveev²⁰, G.L. Melkumov²⁰, A.O. Merzlaya²², B. Messerly²⁹, Ł. Mik¹⁴, G.B. Mills²⁷, S. Morozov^{19,21}, S. Mrówczyński¹⁰, Y. Nagai²⁸, M. Naskret¹⁷, V. Ozvenchuk¹¹, V. Paolone²⁹, M. Pavin^{4,3}, O. Petukhov^{19,21}, C. Pistillo²⁴, R. Płaneta¹³, P. Podlaski¹⁶, B.A. Popov^{20,4}, M. Posiadała¹⁶, D. Prokhorova²², S. Puławski¹⁵, J. Puzović²³, R. Rameika²⁶, W. Rauch⁶, M. Ravonel²⁵, R. Renfordt⁷, E. Richter-Was¹³, D. Röhrich⁹, E. Rondio¹², M. Roth⁵, B.T. Rumberger²⁸, A. Rustamov^{1,7}, M. Rybczynski¹⁰, A. Rybicki¹¹, A. Sadovsky¹⁹, K. Schmidt¹⁵, I. Selyuzhenkov²¹, A.Yu. Seryakov²², P. Seyboth¹⁰, M. Słodkowski¹⁸, A. Snoch⁷, P. Staszal¹³, G. Stefanek¹⁰, J. Stepaniak¹², M. Strikhanov²¹, H. Ströbele⁷, T. Šušar³, A. Taranenko²¹, A. Tefelska¹⁸, D. Tefelski¹⁸, V. Tereshchenko²⁰, A. Toia⁷, R. Tsenov², L. Turko¹⁷, R. Ulrich⁵, M. Unger⁵, F.F. Valiev²², D. Veberič⁵, V.V. Vechernin²², M. Walewski¹⁶, A. Wickremasinghe²⁹, C. Wilkinson²⁴, Z. Włodarczyk¹⁰, A. Wojtaszek-Szwarc¹⁰, O. Wyszynski¹³, L. Zambelli^{4,1}, E.D. Zimmerman²⁸, and R. Zwaska²⁶

¹ National Nuclear Research Center, Baku, Azerbaijan

² Faculty of Physics, University of Sofia, Sofia, Bulgaria

³ Ruđer Bošković Institute, Zagreb, Croatia

⁴ LPNHE, University of Paris VI and VII, Paris, France

⁵ Karlsruhe Institute of Technology, Karlsruhe, Germany

⁶ Fachhochschule Frankfurt, Frankfurt, Germany

⁷ University of Frankfurt, Frankfurt, Germany

⁸ Wigner Research Centre for Physics of the Hungarian Academy of Sciences, Budapest, Hungary

⁹ University of Bergen, Bergen, Norway

¹⁰ Jan Kochanowski University in Kielce, Poland

- ¹¹ H. Niewodniczański Institute of Nuclear Physics of the Polish Academy of Sciences, Kraków, Poland
- ¹² National Centre for Nuclear Research, Warsaw, Poland
- ¹³ Jagiellonian University, Cracow, Poland
- ¹⁴ AGH - University of Science and Technology, Cracow, Poland
- ¹⁵ University of Silesia, Katowice, Poland
- ¹⁶ University of Warsaw, Warsaw, Poland
- ¹⁷ University of Wrocław, Wrocław, Poland
- ¹⁸ Warsaw University of Technology, Warsaw, Poland
- ¹⁹ Institute for Nuclear Research, Moscow, Russia
- ²⁰ Joint Institute for Nuclear Research, Dubna, Russia
- ²¹ National Research Nuclear University (Moscow Engineering Physics Institute), Moscow, Russia
- ²² St. Petersburg State University, St. Petersburg, Russia
- ²³ University of Belgrade, Belgrade, Serbia
- ²⁴ University of Bern, Bern, Switzerland
- ²⁵ University of Geneva, Geneva, Switzerland
- ²⁶ Fermilab, Batavia, USA
- ²⁷ Los Alamos National Laboratory, Los Alamos, USA
- ²⁸ University of Colorado, Boulder, USA
- ²⁹ University of Pittsburgh, Pittsburgh, USA

1 Introduction

NA61/SHINE is a fixed-target experiment [1] operating at the CERN Super-Proton-Synchrotron (SPS). The NA61/SHINE Collaboration studies, in particular, properties of hadron production in nucleus-nucleus collisions. The primary aim is to uncover features of the phase transition between confined matter and quark gluon plasma (QGP). Within the current program, data on p+p, Be+Be, Ar+Sc, Xe+La, and Pb+Pb collisions at beam momenta in the range $13A-150A$ GeV/c has been recorded.

This program was recently extended by measurements of charm hadron production in nucleus-nucleus collisions. The motivation of the charm program is discussed in Sec. 2. The current status of the program including the preliminary results of first data taking campaigns performed in 2016 and 2017 is presented in Sec. 3. The plans of NA61/SHINE for systematic charm measurements in the years 2021 – 2024 are discussed in Sec. 4.

2 Motivation for the charm program

There are a lot of questions that need to be answered concerning charm production in nucleus-nucleus collisions. Among them, there are three that motivate charm measurements by NA61/SHINE:

- (i) What is the mechanism of charm production?
- (ii) How does the onset of deconfinement impact charm production?
- (iii) How does the formation of quark gluon plasma impact J/ψ production?

To answer these questions, knowledge on the mean number of charm quark pairs produced in full phase space in heavy ion collisions, $\langle c\bar{c} \rangle$, is needed. Such data does not exist yet and NA61/SHINE aims to provide them within the coming years.

2.1 Mechanism of charm production

Figure 1 presents a compilation of predictions provided by dynamical and statistical models on $\langle c\bar{c} \rangle$ in central Pb+Pb collisions at $158A$ GeV/c. These predictions are obtained from:

- (i) A pQCD-inspired model [2, 3] - charm data independent calculation based on model assumptions and nucleon pdfs only.
- (ii) The Hadron String Dynamics (HSD) model [4] - a pQCD-inspired extrapolation of p+p data.

- (iii) The Hadron Resonance Gas model (HRG) [5] - a calculation of equilibrium yields of charm hadrons assuming parameters of a hadron resonance gas fitted to mean multiplicities of light hadrons.
- (iv) The Statistical Quark Coalescence model [5] - the mean number of $\langle c\bar{c} \rangle$ pairs is calculated using the measured $\langle J/\psi \rangle$ multiplicity [6] and the probability of a single $c\bar{c}$ pair hadronization into $\langle J/\psi \rangle$ calculated within the model.
- (v) The Dynamical Quark Coalescence model [7] - the mean number of $\langle c\bar{c} \rangle$ pairs is calculated using the measured $\langle J/\psi \rangle$ multiplicity [6] and the probability of a single $c\bar{c}$ pair hadronization into $\langle J/\psi \rangle$ calculated within the model.
- (vi) The Statistical Model of the Early Stage (SMES) [8] - the mean number of charm quarks is calculated assuming an equilibrium QGP at the early stage of the collision.

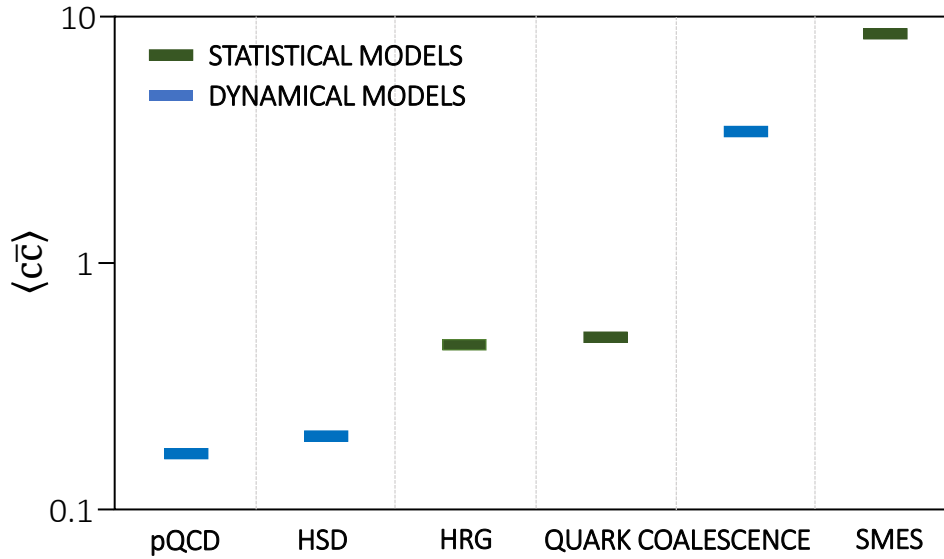


Figure 1: Mean multiplicity of charm quark pairs produced in the full phase space in central Pb+Pb collisions at 158A GeV/c calculated with dynamical models (blue bars): pQCD-inspired [2,3], HSD [4], and Dynamical Quark Coalescence [7], as well as statistical models (green bars): HRG [5], Statistical Quark Coalescence [5], and SMES [8].

The predictions of the models on $\langle c\bar{c} \rangle$ differ by about two orders of magnitude. Therefore, obtaining precise data on $\langle c\bar{c} \rangle$ is expected to allow to narrow the spectrum of viable theoretical models and thus learn about the charm quark and hadron production mechanisms.

2.2 Charm production as a signal of onset of deconfinement

The production of charm is expected to be different in confined and deconfined matter. This is caused by different properties of charm carriers in these phases. In confined matter the lightest charm carriers are D mesons, whereas in deconfined matter the carriers are charm quarks. Production of a $D\bar{D}$ pair ($2m_D = 3.7\text{ GeV}$) requires energy about 1 GeV higher than production of a $c\bar{c}$ pair ($2m_c = 2.6\text{ GeV}$). The effective number of degrees of freedom of charm hadrons and charm quarks is similar [9]. Thus, more abundant charm production is expected in deconfined than in confined matter. Consequently, in analogy to strangeness [8, 10], a change of collision energy dependence of $\langle c\bar{c} \rangle$ may be a signal of onset of deconfinement.

Figures 2 and 3 present collision energy dependence of charm production in central Pb+Pb collisions at $150A\text{ GeV}/c$ predicted by two very different models: the Statistical Model of the Early Stage 2 [9] and a pQCD-inspired model [11], respectively.

Figure 2 shows the energy dependence of $\langle c\bar{c} \rangle$ predicted by the Statistical Model of the Early Stage. According to this model, when crossing the phase transition energy range ($\sqrt{s_{NN}} = 7 - 11\text{ GeV}$), an enhancement of $\langle c\bar{c} \rangle$ production should be observed. At $150A\text{ GeV}/c$ ($\sqrt{s_{NN}} = 16.7\text{ GeV}$) an enhancement by a factor of about 4 is expected.

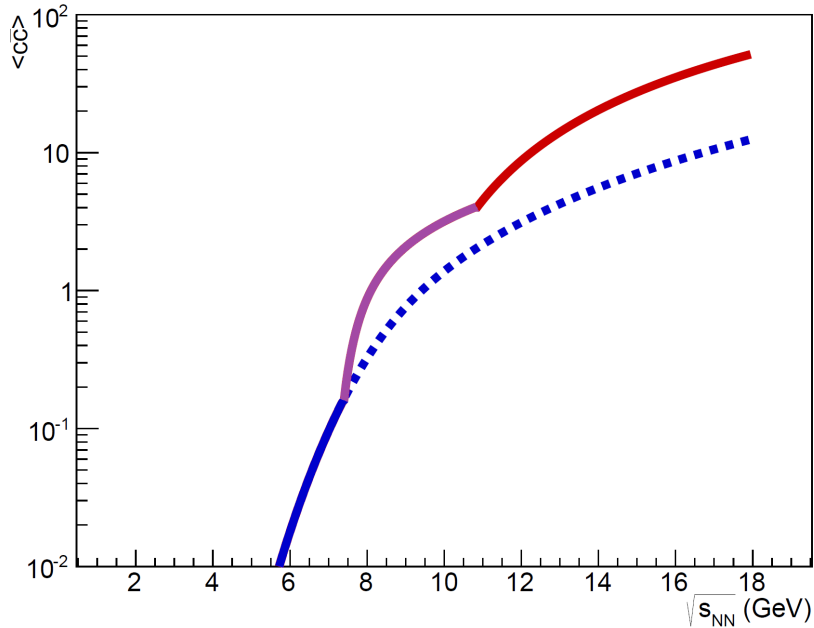


Figure 2: Energy dependence of $\langle c\bar{c} \rangle$ in central Pb+Pb collisions calculated within the SMES model [9, 12]. The blue line corresponds to confined, the purple line to mixed phase, and the red line to deconfined matter. The dashed line presents the prediction without a phase transition.

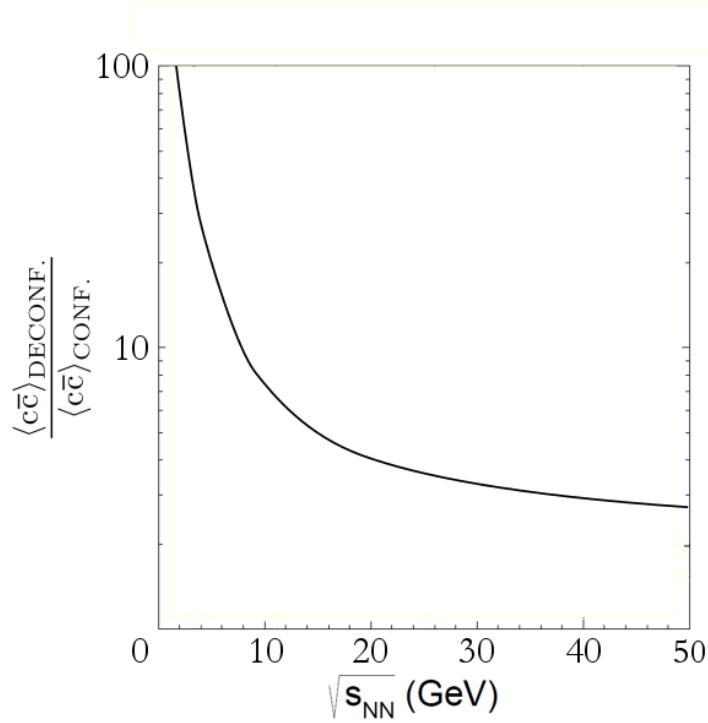


Figure 3: Energy dependence of the ratio of $\langle c\bar{c} \rangle$ in deconfined and confined matter in central Pb+Pb collisions calculated within the pQCD-inspired model of Ref. [11].

Figure 3 shows the ratio of mean multiplicity of $c\bar{c}$ pairs in deconfined and confined matter. Both numerator and denominator were calculated at the same collision energy. At $150A \text{ GeV}/c$ ($\sqrt{s_{\text{NN}}} = 16.7 \text{ GeV}$) an enhancement by a factor of about 3 is predicted.

Accurate experimental results will allow to test these predictions.

2.3 J/ψ production as a signal of deconfinement

Suppression of the production of J/ψ mesons in central Pb+Pb collisions at $158A \text{ GeV}/c$ was an important argument for the CERN announcement of the discovery of a new state of matter [13]. Within the Matsui-Satz model [14] the suppression is supposed to be caused by the formation of the QGP.

Figure 4 presents two scenarios of charmonium production. In the first case (Fig. 4 (left)), a produced $c\bar{c}$ pair hadronizes in a vacuum – this corresponds to a p+p interaction. Open charm and charmonia are produced in vacuum with a certain probability, at high collision energies typically 10% of $c\bar{c}$ pairs form charmonia and 90% appear in charm hadrons.

The second scenario is presented in Fig. 4 (right). Here the $c\bar{c}$ pair forms a pre-charmonium state in the quark gluon plasma. Due to the color screening, which may lead to disintegration of this state, the probability of charmonium production is suppressed in favor of open charm production.

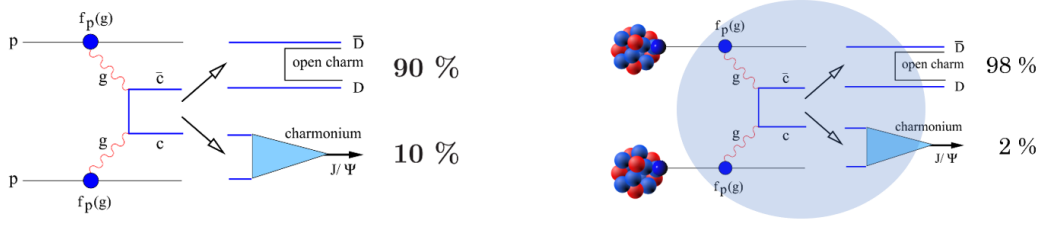


Figure 4: Sketch of the J/ψ production mechanism and its relation to $c\bar{c}$ production in p+p interactions (*left*) and central heavy ion collisions (*right*) [15].

The probability of a $c\bar{c}$ pair hadronizing to J/ψ is defined as:

$$P(c\bar{c} \rightarrow J/\psi) \equiv \frac{\langle J/\psi \rangle}{\langle c\bar{c} \rangle} \equiv \frac{\sigma_{J/\psi}}{\sigma_{c\bar{c}}}. \quad (1)$$

To be able to calculate this probability, one needs data on both J/ψ and $c\bar{c}$ yields in the full phase space. At the CERN SPS precise $\langle J/\psi \rangle$ data was provided by the NA38 [16], NA50 [6], and NA60 [17] experiments, while $\langle c\bar{c} \rangle$ data is not available at the CERN SPS up to now.

The problem of the lack of the $\langle c\bar{c} \rangle$ data was worked around [6,14] by assuming that the mean multiplicity of $c\bar{c}$ pairs is proportional to the mean multiplicity of Drell-Yan pairs: $\langle c\bar{c} \rangle \sim \langle DY \rangle$.

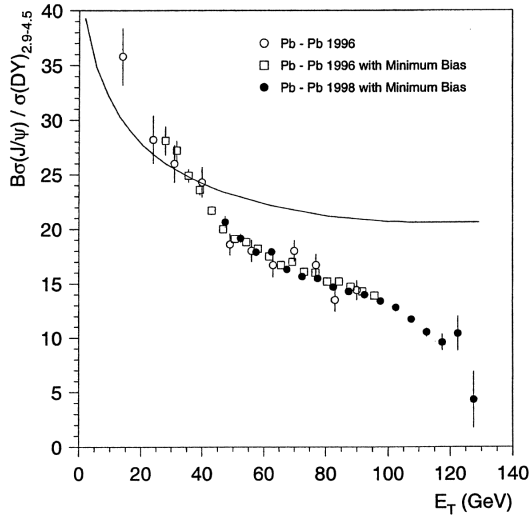


Figure 5: The ratio of $\sigma_{J/\psi}/\sigma_{DY}$ as a function of transverse energy in Pb+Pb collisions at 158A GeV measured by NA50. The curve represents the J/ψ suppression due to ordinary nuclear absorption [6].

Figure 5 shows the result from the NA50 experiment [6] that was interpreted, basing on this assumption, as an evidence for QGP creation in central Pb+Pb collisions at $158A$ GeV. However, the assumption $\langle c\bar{c} \rangle \sim \langle DY \rangle$ may be incorrect due to many effects, such as shadowing or parton energy losses [18].

This clearly shows a need for precise data on $\langle c\bar{c} \rangle$. NA61/SHINE has recently started such measurements.

3 First measurements of open charm in NA61/SHINE

Precise measurements of charm hadron production by NA61/SHINE should be performed in 2021-2024. The related preparations have started already. In 2015 and 2016, a Small Acceptance Vertex Detector was constructed and the first measurements of open charm has been started in 2016.

3.1 Small Acceptance Vertex Detector

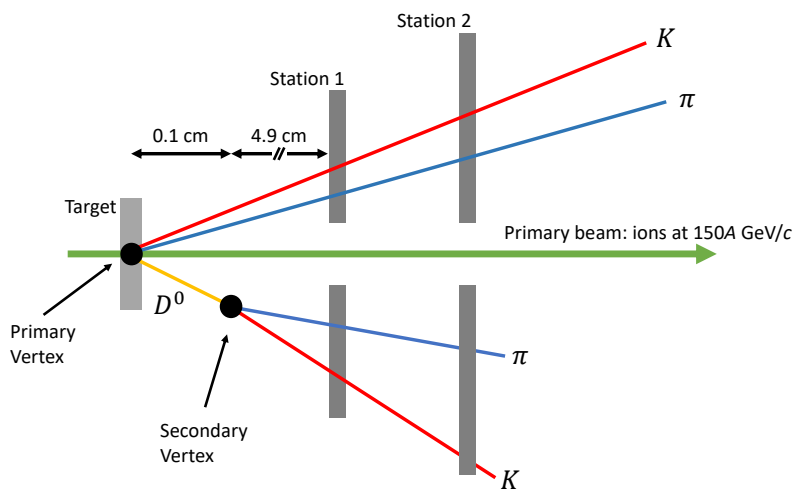


Figure 6: Schematics of reconstruction of a $D^0 \rightarrow \pi^+ + K^-$ decay with help of a vertex detector.

Starting the open charm program required construction of a new high-resolution vertex detector. Its role in measurements of charm hadrons is schematically shown in Fig. 6.

This measurement is challenging due to the short mean lifetime of charm hadrons and the relatively low branching ratios into reconstructable decay channels. Table 1

presents properties of the more frequently produced charm hadrons relevant to their measurement.

Table 1: The most frequently produced charm hadrons: their mass, mean life time, and best suited decay channels for measurements are shown.

Hadron	Decay channel	$c\bar{\tau}$ [μm]	BR
D^0	$\pi^+ + K^-$	123	3.89%
D^+	$\pi^+ + \pi^+ K^-$	312	9.22%
D_s^+	$\pi^+ + K^- + K^+$	150	5.50%
Λ_c	$p + \pi^+ + K^-$	60	5.00%

A big upside of NA61/SHINE is the fact, that this is a fixed-target experiment. Due to the Lorenz boost ($\beta\gamma \approx 10$ at midrapidity and $p_T \approx 0$), the average separation between the primary and the decay vertices of D^0 mesons is about 1 mm. This makes the measurement significantly easier than in the case of collider experiments. In addition, due to the fact that magnetic field is perpendicular to the beam direction (unlike in a typical collider experiment, where it is parallel to the beam direction), the acceptance extends to $p_T = 0$.

For the measurement of D^0 mesons, the Small Acceptance Vertex Detector (SAVD) was added to the NA61/SHINE detector in October 2016. It's location in the NA61/SHINE detector is shown in Fig. 7.

The SAVD was built using sixteen CMOS MIMOSA-26 sensors [19]. The basic sensor properties are:

- (i) $18.4 \times 18.4 \mu\text{m}^2$ pixels,
- (ii) 115 μs time resolution,
- (iii) $10 \times 20 \text{mm}^2$ surface, 0.66 MPixel,
- (iv) 50 μm thick.

The estimated material budget per layer is 0.3% of the radiation length.

The sensors were glued to eight ALICE ITS ladders [20], which were mounted on two horizontally movable arms and spaced by 5 cm along the z (beam) direction. The detector box was filled with He (to reduce beam-gas interactions) and contained an integrated target holder to avoid unwanted material and multiple coulomb scattering between target and detector.

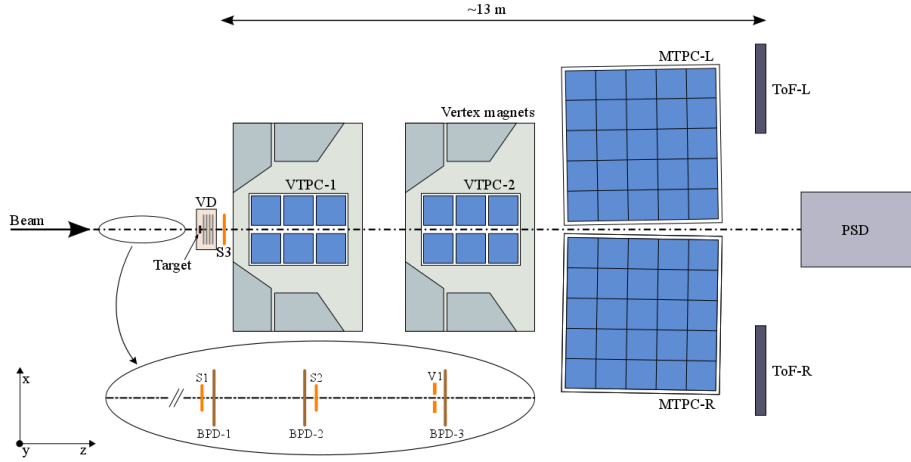


Figure 7: Schematic layout of the NA61/SHINE experiment at the CERN SPS (horizontal cut in the beam plane, not to scale). The beam and trigger counter configuration used for data taking on Pb+Pb collisions in 2016 is presented. The chosen right-handed coordinate system is shown on the plot. The incoming beam direction is along the z axis. The Small Acceptance Vertex Detector together with the integrated target station is located upstream of the VTPC-1.

The simulations of SAVD performance using the AMPT physics input [21] has shown that about 4% [22] of all $D^0 \rightarrow \pi^+ + K^-$ decays will be reconstructed and accepted by the analysis cuts. Figure 8 shows the phase space coverage which the SAVD provides.

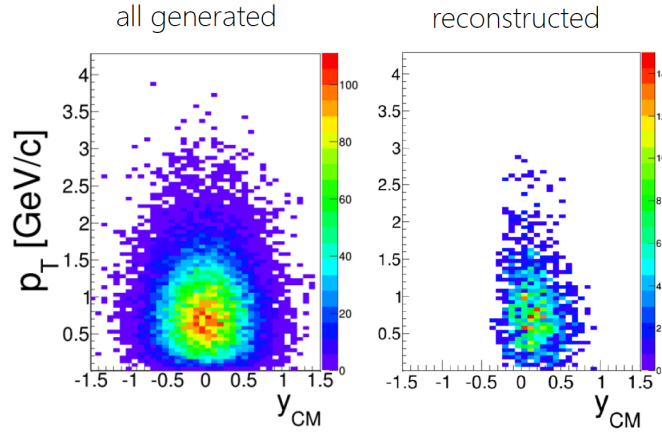


Figure 8: The AMPT model simulation of transverse momentum and rapidity distributions of D^0 mesons produced central Pb+Pb collisions at $150A$ GeV/c corresponding to $4 \cdot 10^6$ events. *Left:* all produced D^0 mesons. *Right:* D^0 mesons fulfilling the following criteria: decay into $D^0 \rightarrow \pi^+ + K^-$, both decay products registered by the SAVD, and passing background suppression and quality cuts [22].

3.2 Test data taking in 2016: Pb+Pb central collisions at 150A GeV/c

The SAVD was used in December 2016 during a Pb+Pb test run. Data on central Pb+Pb collisions at 150A GeV/c were collected. Using these data, the following was demonstrated:

- (i) tracking in a large track multiplicity environment,
- (ii) precise primary vertex reconstruction,
- (iii) TPC and SAVD track matching,
- (iv) feasibility to search for the D^0 and \bar{D}^0 signals.

Based on these data, the spatial resolution of the SAVD was determined. Cluster position resolution is $\sigma_{x,y}(Cl) \approx 5 \mu\text{m}$ and primary vertex resolution in the transverse plane is $\sigma_x(PV) \approx 5 \mu\text{m}$, $\sigma_y(PV) \approx 1.8 \mu\text{m}^2$, and along the beam direction is $\sigma_z(PV) \approx 30 \mu\text{m}$ for a typical multiplicity of events recorded in 2016. Primary vertex resolution of $30 \mu\text{m}$ is sufficient to perform the search for the D^0 and \bar{D}^0 signals. Figure 9 shows the first indication of a D^0 and \bar{D}^0 peak obtained using the data collected during the Pb+Pb run in 2016.

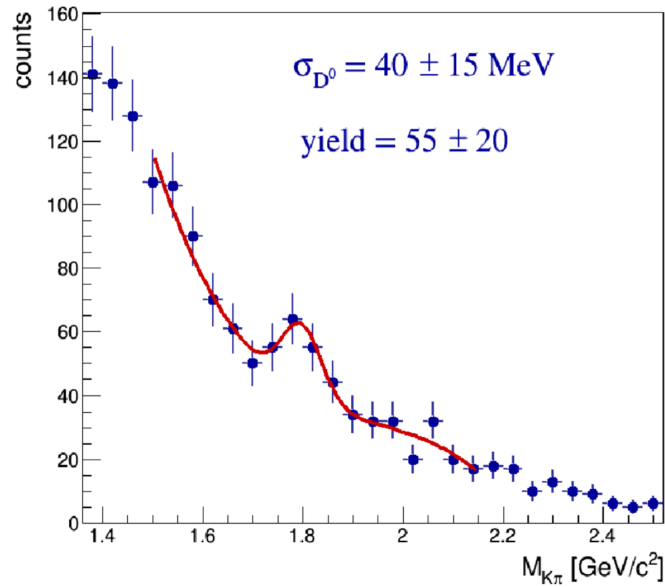


Figure 9: The invariant mass distribution of D^0 and \bar{D}^0 candidates in central Pb+Pb collisions at 150A GeV/c after the background suppression cuts. The particle identification capability of NA61/SHINE was not used at this stage of the analysis [22].

² $\sigma_x(PV) > \sigma_y(PV)$ because $B_y \gg B_x$

3.3 Data taking in 2017 and 2018

Successful performance of the SAVD in 2016 led to the decision to also use it during the Xe+La data taking in 2017. About $5 \cdot 10^6$ events on central Xe+La collisions at $150A \text{ GeV}/c$ were collected in October and November 2017.

To get a first estimate of the number of D^0 and \bar{D}^0 decays that can be reconstructed in this data set, simulations for Pb+Pb collisions and p-QCD inspired system size dependence were combined. Based on these simulations, one expects to reconstruct several hundred of D^0 and \bar{D}^0 decays. This would be in itself an important physics result.

Moreover, one could combine this measurements with published results on J/ψ production. The NA60 experiment [17] measured J/ψ production in In+In collisions (Fig. 10), which is a system of similar size as Xe+La. This combination of the NA60 data on J/ψ and the NA61/SHINE results on open charm could already challenge theoretical models.

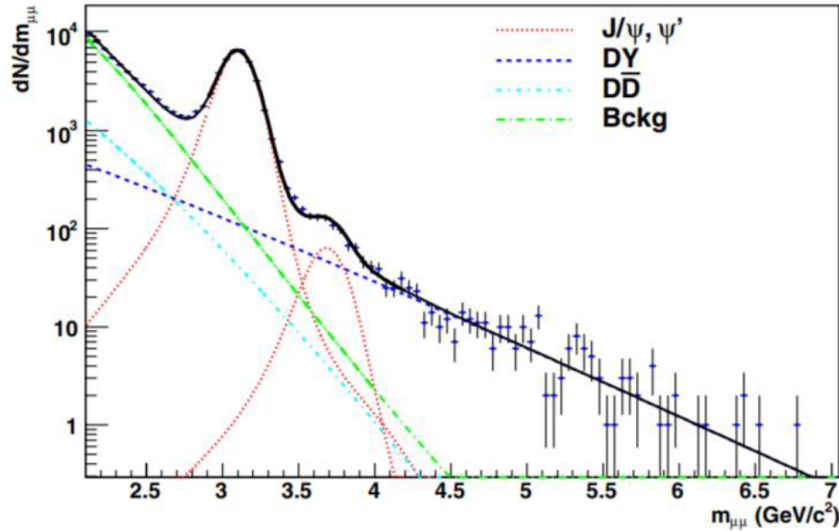


Figure 10: The invariant mass distribution of $\mu^+ \mu^-$ pairs produced in In+In collisions at $158A \text{ GeV}/c$ showing a strong peak due to J/ψ decays [17].

The SAVD is also planned to be used during three weeks of the Pb+Pb data taking in 2018 (recommended by the CERN SPS Committee in October 2017). About $1 \cdot 10^7$ central collisions should be recorded and 4000 D^0 and \bar{D}^0 decays can be expected to be reconstructed in this data set. The expected signal to background ratio is about 2.6 with realistic PID.

4 Systematic studies of charm by NA61/SHINE

Precise open charm measurements in NA61/SHINE are planned for the years 2021-2024. They will include measurements in central Pb+Pb collisions at $40A$ GeV/ c and $150A$ GeV/ c , in mid-central and peripheral Pb+Pb collisions at $150A$ GeV/ c , and reconstruction of decays of various open charm mesons (see Table 1).

4.1 NA61/SHINE upgrades

During the Long Shutdown 2 at CERN (2019-2020), a significant upgrade of the NA61/SHINE spectrometer is planned (Fig. 11), in order to allow precise charm measurements.

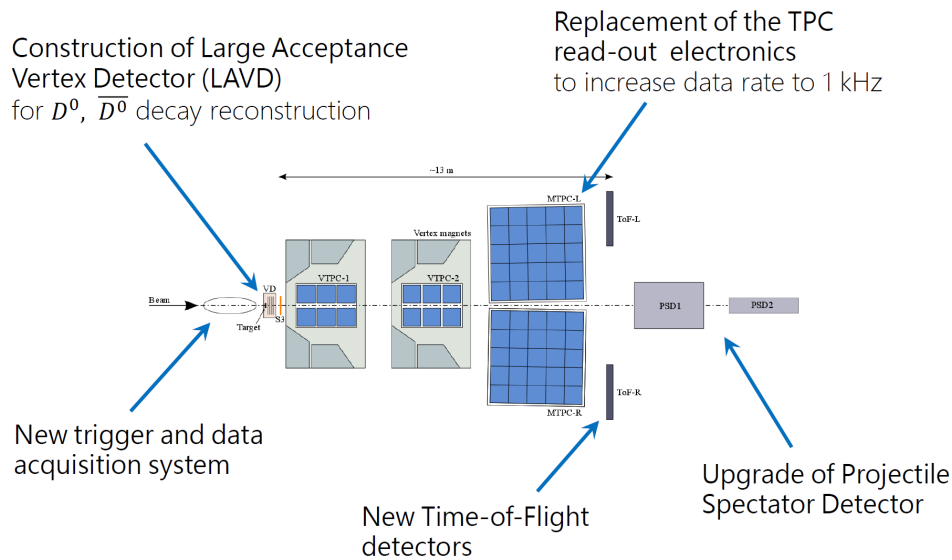


Figure 11: Upgrades of NA61/SHINE planned to be completed during the LS2 period.

The most important upgrade from the open charm point of view is the construction of a new vertex detector: the Large Acceptance Vertex Detector (LAVD). Also, for obtaining higher data rate (1 kHz) the TPC electronics will be replaced and a new trigger and data acquisition system will be built. An upgrade of the Projectile Spectator Detector will also be performed to cope with the higher beam intensity expected to be delivered after LS2. Finally, new ToF detectors are planned to be constructed to improve particle identification at mid-rapidity.

4.2 Large Acceptance Vertex Detector

To improve the quality of open charm measurement, the Large Acceptance Vertex Detector will replace the existing SAVD detector. The LAVD will be constructed using technology developed for the ALICE ITS: CMOS ALPIDE pixel sensors, carbon fiber support structures, and read-out electronics [23]. Basic properties of the ALPIDE sensors are: $28 \times 28 \mu\text{m}$ pixels, less than $10 \mu\text{s}$ time resolution, $15 \times 30 \text{mm}^2$ surface, 0.5 MPixel, and $50 \mu\text{m}$ thickness.

The estimated material budget per layer is 0.3% of the radiation length. The detector will consist of 4 stations. The transverse dimensions of the stations are: $2 \times 4 \text{cm}^2$ for the first station, $4 \times 8 \text{cm}^2$ for the second, $6 \times 12 \text{cm}^2$ for the third, and $8 \times 16 \text{cm}^2$ for the fourth station. Each station has a square beam hole of $(3 \times 3 \text{mm}^2)$ in the center. The LAVD area will be covered by 126 sensors.

The beam request related to the open charm measurements in 2022-2024 is shown in Table 2.

Table 2: The NA61/SHINE beam request related to the charm program.

Year	Beam	Duration	Purpose	$D^0 + \bar{D}^0$ stat.
2021	p at 150A GeV/c	4 weeks	detector commissioning and tests	
2022	Pb at 150A GeV/c	2 weeks	charm in central collisions	40k
2022	Pb at 150A GeV/c	4 weeks	charm in peripheral collisions	8k
2023	Pb at 150A GeV/c	2 weeks	charm in mid-central collisions	20k
2024	Pb at 40A GeV/c	4 weeks	charm in central collisions	2k

With the upgraded NA61/SHINE spectrometer, one expects that during two weeks of data taking in 2022, $4 \cdot 10^7$ central Pb+Pb collisions at 150A GeV/c will be collected and $4 \cdot 10^4 D^0$ and \bar{D}^0 decays will be reconstructed.

The expected high statistics of reconstructed D^0 and \bar{D}^0 decays is due to the high event rate and the large acceptance of the LAVD. Its acceptance will be about 12% (three times better than for the SAVD) of all the D^0 in the $\pi^+ + K^-$ decay channel. Moreover, based on AMPT simulations one estimates that fully corrected results will correspond to more than 90% of the D^0 and \bar{D}^0 yield (see Fig. 12). Total systematic uncertainty of $\langle D^0 \rangle$ and $\langle \bar{D}^0 \rangle$ is expected to be about 10%.

4.3 Charm program: anticipated results

The data obtained by NA61/SHINE should lead to unique and important results on charm production in heavy ion collisions.

Figure 13 presents a compilation of present and future facilities and their region of coverage in the phase diagram of strongly interacting matter. Their capability to measure charm hadrons is summarized below:

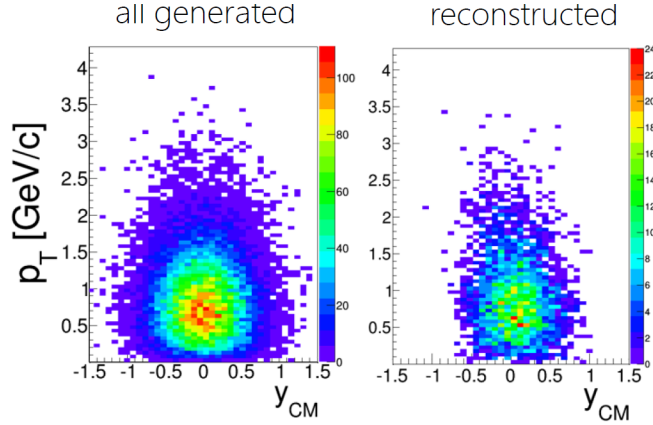


Figure 12: The AMPT simulation of transverse momentum and rapidity distributions of D^0 mesons produced in central Pb+Pb collisions at 150A GeV/c corresponding to $4 \cdot 10^6$ events. *Left:* all produced D^0 mesons. *Right:* D^0 mesons fulfilling the following criteria: decay into $D^0 \rightarrow \pi^+ + K^-$, decay products registered by the LAVD, and passing background suppression and quality cuts [22].

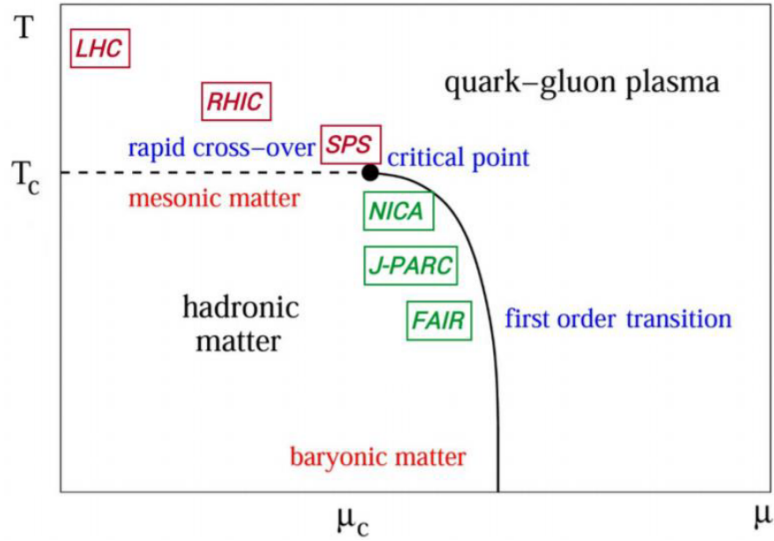


Figure 13: Present (red) and future (green) heavy ion facilities in the phase diagram of strongly interacting matter.

- (i) LHC and RHIC at high energies ($\sqrt{s_{NN}} \gtrsim 200$ GeV): measurements of open charm is performed in limited acceptance; this is due to the collider kinematics and related to the detector geometry [24–27].
- (ii) RHIC BES collider ($\sqrt{s_{NN}} = 7.7 - 39$ GeV): measurement not considered in the current program, this may be likely due to difficulties related to collider geometry

and kinematics as well as the low charm production cross-section [28,29].

- (iii) RHIC BES fixed-target ($\sqrt{s_{NN}} = 3 - 7.7$ GeV): not considered in the current program [30].
- (iv) NICA ($\sqrt{s_{NN}} < 11$ GeV): measurements during the stage 2 (after 2023) are under consideration [31,32].
- (v) J-PARC-HI ($\sqrt{s_{NN}} \lesssim 6$ GeV): under consideration, may be possible after 2025 [33, 34].
- (vi) FAIR SIS-100 ($\sqrt{s_{NN}} \lesssim 5$ GeV): not possible due to the very low cross-section at SIS-100, systematic charm measurements are planned with SIS-300 ($\sqrt{s_{NN}} \lesssim 7$ GeV) which is agreed-on part of FAIR, but not of the start version (timeline is unclear) [35,36].

The conclusion is that only NA61/SHINE is able to measure open charm production in heavy ion collisions in full phase space in the near future.

Having this data, one can try to answer the motivating questions.

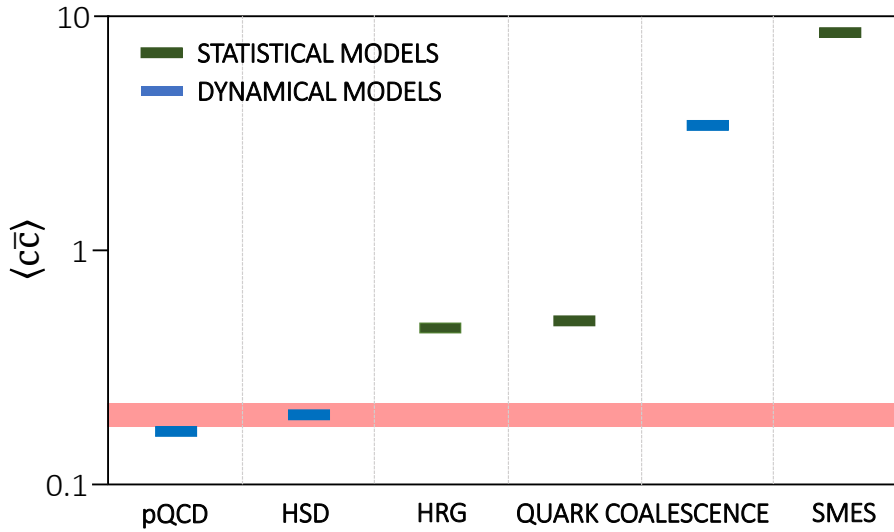


Figure 14: Mean multiplicity of charm quark pairs produced in central Pb+Pb collisions at $158A$ GeV/ c calculated within dynamical models (blue bars) and statistical models (green bars). The width of the red band, at the location assuming HSD predictions, indicates the accuracy of the NA61 2020+ result.

Figure 14 shows a foreseen accuracy of NA61/SHINE data on mean charm multiplicity in reference to charm production models (see Sec. 2 for details). The red band

indicates the foreseen accuracy of NA61/SHINE result on the charm yield assuming the yield prediction of the HSD model [4]. With that accuracy it should be possible to exclude most of the current models.

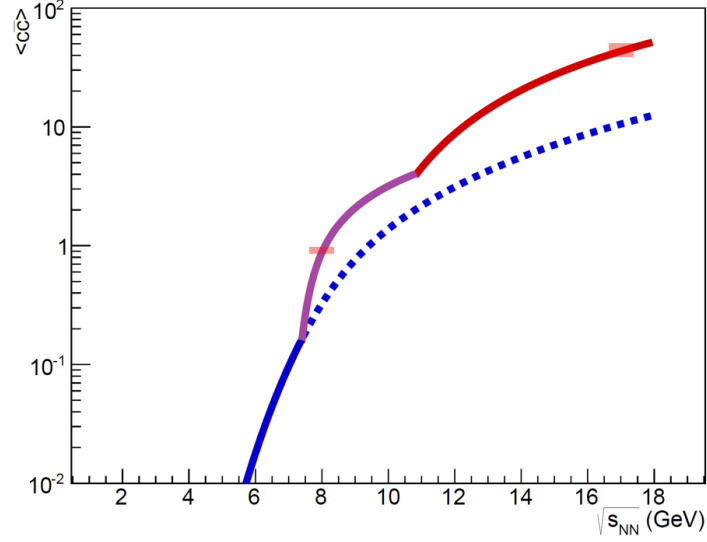


Figure 15: Energy dependence of $\langle c\bar{c} \rangle$ in central Pb+Pb collisions calculated within the SMES model. The red bars indicate the accuracy of NA61 2020+ results for two energies: $40A$ GeV/ c ($\sqrt{s_{NN}} = 8.6$ GeV) and $150A$ GeV/ c ($\sqrt{s_{NN}} = 16.7$ GeV), assuming the SMES yields [8].

Figure 15 shows a foreseen accuracy of NA61/SHINE data on $\langle c\bar{c} \rangle$ in reference to SMES predictions (see Sec. 2 for details). Red bars indicate the foreseen accuracy of the NA61/SHINE result on charm multiplicity for energies included in the proposed NA61/SHINE charm studies: $40A$ GeV/ c ($\sqrt{s_{NN}} = 8.6$ GeV) and $150A$ GeV/ c ($\sqrt{s_{NN}} = 16.7$ GeV). These points would be a start of confronting model predictions on collision energy dependence, but measurements at more energies are necessary. In the future, this can be performed at J-PARC-HI and FAIR SIS-300.

Figure 16 shows a foreseen accuracy of NA61/SHINE data on charm in reference to J/ψ suppression (see Sec. 2 for details). The red bars indicate the foreseen accuracy of the $\sigma_{J/\psi}/\sigma_{c\bar{c}}$ result that was made assuming $\sigma_{c\bar{c}} \sim \sigma_{\pi}$. One will be able to distinguish between two extreme scenarios: $\langle c\bar{c} \rangle \sim \langle DY \rangle$ or $\langle c\bar{c} \rangle \sim \langle \pi \rangle$.

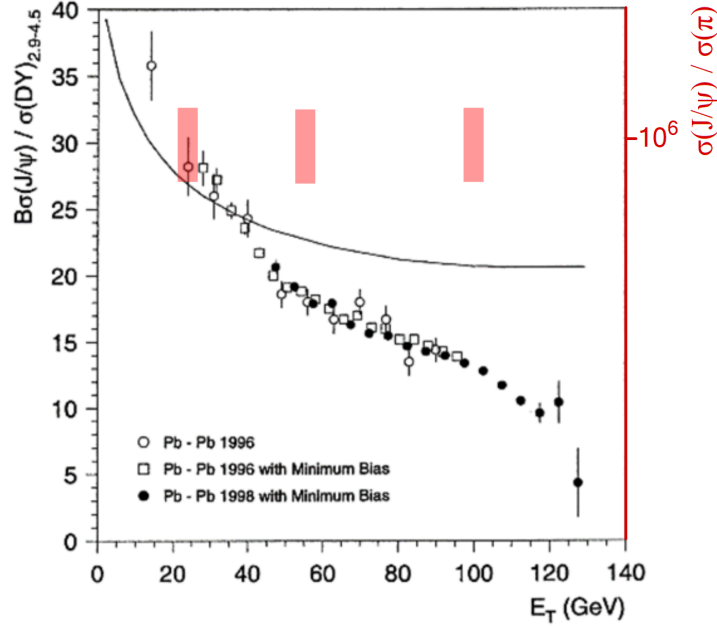


Figure 16: The ratio of $\sigma_{J/\psi}/\sigma_{DY}$ (left) and $\sigma_{J/\psi}/\sigma_{\pi}$ (right) as a function of transverse energy in Pb+Pb collisions at 158A GeV. The $\sigma_{J/\psi}/\sigma_{DY}$ ratio was measured by NA50 [6] and it was used to calculate the $\sigma_{J/\psi}/\sigma_{\pi}$ ratio in Ref. [37]. Red bars mark the $\sigma_{J/\psi}/\sigma_{c\bar{c}}$ accuracy of the NA61 2020+ result assuming $\sigma_{c\bar{c}} \sim \sigma_{\pi}$ and scaling to $\sigma_{J/\psi}/\sigma_{DY}$ for peripheral collisions.

5 Summary

NA61/SHINE has started measurements of open charm production in 2017 with data taking on Xe+La collisions at 150A GeV/c. The measurements in central Pb+Pb collisions at 150A GeV/c will be performed in 2018. This has been possible due to an implementation of the silicon pixel Vertex Detector. During the Long Shutdown 2, NA61/SHINE plans to construct the Large Acceptance Vertex Detector and increase the data taking rate by a factor of 10, to 1 kHz.

This will allow to collect high statistics data on open charm hadron production in central Pb+Pb collisions at 150A GeV/c and 40A GeV/c and centrality selected Pb+Pb collisions at 150A GeV/c. The results are expected to:

- (i) distinguish between many existing models of open charm production in Pb+Pb collisions,
- (ii) initiate a measurement of collision energy dependence of open charm yield, which may lead to an observation of open charm signal of the onset of deconfinement,
- (iii) verify J/ψ signal of the QGP formation by measurements of centrality dependence of charm production.

Acknowledgments

We would like to thank Elena Bratkovskaya, Giuseppe Bruno, Mark Gorenstein, Paolo Martinengo, Roman Poberezhnyuk, and Taesoo Song for the information, comments and support that helped to prepare this document.

This work was supported by the Hungarian Scientific Research Fund (Grants NK-FIH 123842–123959), the János Bolyai Research Scholarship of the Hungarian Academy of Sciences, the Polish Ministry of Science and Higher Education (grants 667/N-CERN/2010/0, NN 202 48 4339 and NN 202 23 1837), the Polish National Center for Science (grants 2011/03/N/ST2/03691, 2013/11/N/ST2/03879, 2014/13/N/ST2/02565, 2014/14/E/ST2/00018, 2014/15/B/ST2/02537 and 2015/18/M/ST2/00125, 2015/19/N/ST2/01689), the Foundation for Polish Science — MPD program, co-financed by the European Union within the European Regional Development Fund, the Federal Agency of Education of the Ministry of Education and Science of the Russian Federation (SPbSU research grant 11.38.242.2015), the Russian Academy of Science and the Russian Foundation for Basic Research (grants 08-02-00018, 09-02-00664 and 12-02-91503-CERN), the Ministry of Science and Education of the Russian Federation, grant No. 3.3380.2017/4.6, the National Research Nuclear University MEPhI in the framework of the Russian Academic Excellence Project (contract No. 02.a03.21.0005, 27.08.2013), the Ministry of Education, Culture, Sports, Science and Technology, Japan, Grant-in-Aid for Scientific Research (grants 18071005, 19034011, 19740162, 20740160 and 20039012), the German Research Foundation (grant GA 1480/2-2), the EU-funded Marie Curie Outgoing Fellowship, Grant PIOF-GA-2013-624803, the Bulgarian Nuclear Regulatory Agency and the Joint Institute for Nuclear Research, Dubna (bilateral contract No. 4418-1-15/17), Bulgarian National Science Fund (grant DN08/11), Ministry of Education and Science of the Republic of Serbia (grant OI171002), Swiss Nationalfonds Foundation (grant 200020-117913/1), ETH Research Grant TH-01 07-3 and the U.S. Department of Energy.

References

- [1] N. Abgrall *et al.*, [NA61/SHINE Collab.] *JINST* **9** (2014) P06005, arXiv:1401.4699 [physics.ins-det].
- [2] R. V. Gavai, S. Gupta, P. L. McGaughey, E. Quack, P. V. Ruuskanen, R. Vogt, and X.-N. Wang *Int. J. Mod. Phys. A* **10** (1995) 2999, arXiv:hep-ph/9411438 [hep-ph].
- [3] P. Braun-Munzinger and J. Stachel *Phys. Lett.* **B490** (2000) 196, arXiv:nucl-th/0007059 [nucl-th].
- [4] O. Linnyk, E. L. Bratkovskaya, and W. Cassing *Int. J. Mod. Phys. E* **17** (2008) 1367, arXiv:0808.1504 [nucl-th].
- [5] A. P. Kostyuk, M. I. Gorenstein, H. Stoecker, and W. Greiner *Phys. Lett.* **B531** (2002) 195, arXiv:hep-ph/0110269 [hep-ph].
- [6] M. C. Abreu *et al.*, [NA50 Collab.] *Phys. Lett.* **B477** (2000) 28–36.
- [7] P. Levai, T. S. Biro, P. Csizmadia, T. Csorgo, and J. Zimanyi *J. Phys. G* **27** (2001) 703, arXiv:nucl-th/0011023 [nucl-th].
- [8] M. Gazdzicki and M. I. Gorenstein *Acta Phys. Polon.* **B30** (1999) 2705, arXiv:hep-ph/9803462 [hep-ph].
- [9] R. V. Poberezhnyuk, M. Gazdzicki, and M. I. Gorenstein *Acta Phys. Polon.* **B48** (2017) 1461, arXiv:1708.04491 [nucl-th].
- [10] J. Rafelski and B. Muller *Phys. Rev. Lett.* **48** (1982) 1066. [Erratum: *Phys. Rev. Lett.* 56,2334(1986)].
- [11] A. P. Kostyuk, M. I. Gorenstein, and W. Greiner *Phys. Lett.* **B519** (2001) 207–211, arXiv:hep-ph/0103057 [hep-ph].
- [12] p. c. R. V. Poberezhnyuk.
- [13] U. W. Heinz and M. Jacob arXiv:nucl-th/0002042 [nucl-th].
- [14] T. Matsui and H. Satz *Phys. Lett.* **B178** (1986) 416–422.
- [15] H. Satz *Adv. High Energy Phys.* **2013** (2013) 242918.
- [16] M. C. Abreu *et al.*, [NA50, NA38 Collab.] *Eur. Phys. J.* **C14** (2000) 443–455.
- [17] R. Arnaldi *et al.*, [NA60 Collaboration Collab.] *Phys. Rev. Lett.* **99** (Sep, 2007) 132302. <https://link.aps.org/doi/10.1103/PhysRevLett.99.132302>.
- [18] H. Satz *EPJ Web Conf.* **71** (2014) 00118.
- [19] “Mimosa26 user manual.” https://www.google.de/url?sa=t&rct=j&q=&esrc=s&source=web&cd=1&cad=rja&uact=8&ved=0ahUKEwi4udLhu0HYAhWE1iwKHQ5QC38QFggnMAA&url=http%3A%2F%2Fwww.iphc.cnrs.fr%2FIMG%2Fpdf%2FM26_UserManual_light.pdf&usg=AOvVaw3TtHsmtXtnF057_rFSqXIM.
- [20] B. Abelev *et al.*, [ALICE Collaboration Collab.], “Technical Design Report for the Upgrade of the ALICE Inner Tracking System,” Tech. Rep. CERN-LHCC-2013-024. ALICE-TDR-017, Nov, 2013. <https://cds.cern.ch/record/1625842>.
- [21] Z.-W. Lin *et al.* *Phys. Rev.* **C72** (2005) 064901.
- [22] A. Aduszkiewicz *et al.*, [NA61/SHINE Collaboration Collab.], “Beam momentum scan with Pb+Pb collisions,” Tech. Rep. CERN-SPSC-2015-038. SPSC-P-330-ADD-8, CERN, Geneva, Oct, 2015. <https://cds.cern.ch/record/2059811>.
- [23] G. Aglieri Rinella, [ALICE Collab.] *Nucl. Instrum. Meth.* **A845** (2017) 583.

- [24] E. Meninno, [ALICE Collab.] *EPJ Web Conf.* **137** (2017) 06018.
- [25] G. W. S. Hou, [ATLAS, CMS Collab.] *PoS CHARM2016* (2016) 088.
- [26] M. Simko, [STAR Collab.] *J. Phys. Conf. Ser.* **832** no. 1, (2017) 012028.
- [27] K. Nagashima, [PHENIX Collab.] *Nucl. Phys.* **A967** (2017) 644–647, arXiv:1704.04731 [nucl-ex].
- [28] G. Odyniec *J. Phys. Conf. Ser.* **455** (2013) 012037.
- [29] C. Yang, [STAR Collab.] *Nucl. Phys.* **A967** (2017) 800.
- [30] K. C. Meehan, [STAR Collab.] *Nucl. Phys.* **A956** (2016) 878.
- [31] V. Kekelidze, A. Kovalenko, R. Lednicky, V. Matveev, I. Meshkov, A. Sorin, and G. Trubnikov *Nucl. Phys.* **A967** (2017) 884.
- [32] V. Kekelidze, “Why are we building the nica ?.” <https://indico.cern.ch/event/638553/contributions/2771587/attachments/1554737/2444516/KekelidzeNICAdays.pdf>.
- [33] H. Sako *et al.*, [J-PARC Heavy-Ion Collab.] *Nucl. Phys.* **A956** (2016) 850.
- [34] M. Kitazawa, “Search for qcd critical point at j-parc-hi.” <https://kds.kek.jp/indico/event/25425/session/7/contribution/20>.
- [35] B. Friman, C. Hohne, J. Knoll, S. Leupold, J. Randrup, R. Rapp, and P. Senger *Lect. Notes Phys.* **814** (2011) 1.
- [36] V. Friese, “Studying dense matter with the cbm experiment.” http://www.ectstar.eu/sites/www.ectstar.eu/files/talks/ECT_Nov17_Friese.pdf.
- [37] M. Gazdzicki *Phys. Rev.* **C60** (1999) 054903, arXiv:hep-ph/9809412 [hep-ph].